Prediction and understanding of the north-south displacement of the heliospheric current sheet

X. P. Zhao, J. T. Hoeksema and P. H. Scherrer
W. W. Hansen Experimental Physics Laboratory, Stanford University, USA

Short title: NORTH-SOUTH DISPLACEMENT OF HELIOSPHERIC CURRENT SHEET

Abstract. Based on WSO observations of the photospheric magnetic field and the potential field-source surface (PFSS) model, we compare the solid angles occupied by the positive source surface field with that of the negative. We develop an algorithm to quantitatively estimate and understand the positive-negative displacement of the heliospheric current sheet (HCS) about Sun's magnetic dipole equator and the north-south displacement of the HCS about the heliographic equator. The north-south HCS displacement predicted using the algorithm quantitatively agrees with that observed by Ulysses and WIND in 1994-1995. The predicted positive-negative and north-south HCS displacement for 362 Carrington rotations between 1976 and 2001 show that in addition to the two long southward HCS displacement intervals that are consistent with earlier observations and statistical results, there are several short north-south HCS displacement intervals in the rising and early declining solar activity phases. All the positive-negative HCS displacements about the Sun's magnetic dipole equator determined for the 25 years can be understood using the positive-negative asymmetry in the characteristics of coronal holes or open field regions between two hemispheres, such as the area, field strength or the outward expansion factor of the coronal holes. To understand the north-south HCS displacement about the heliographic equator, the effect of the Sun's magnetic dipole tilt angle relative to the Sun's rotation axis must be taken into consideration as well.

1. Introduction

The initial observation of the sector structure and sector boundaries [*Wilcox and Ness*, 1965] led to the recognition of the existence of the heliospheric current sheet (HCS), a surface that separates the heliosphere into two magnetic hemispheres with opposite magnetic polarity [*Schulz*, 1973]. Based on the small annual excursion of the Earth's heliographic latitude, the detection of the heliographic latitude dependence in the dominant polarity of the heliospheric magnetic field (HMF) near the Earth has been used to determine the morphology of the HCS. The north-south HCS displacement from the heliographic equator was one of the major topics in the early study of the HCS configuration (especially before the middle of 1980s), though the conclusions are somewhat ambiguous [*Tritakis*, 1984 and the references therein].

The first simple HCS model is a tilted dipole equator [*Schulz*, 1973; *Hundhausen*, 1977; *Smith, Tsurutani and Rosenberg*, 1978], i.e., a sinusoidal HCS symmetric about the heliographic equator. This geometry was introduced based on the observation of the sinusoidal heliographic latitude dependence of the duration of the dominant HMF polarity sectors in the ascending phase of the solar activity cycle [*Rosenberg and Coleman*, 1969]. The observation of the latitudinal variation of dominant polarities in the maximum and early declining phases, which was basically sinusoidal but asymmetric about the heliographic equator, led to the introduction of an asymmetric, sinusoidal HCS model for the HCS around solar activity maximum [*Rosenberg*, 1970; 1975].

However, by analyzing the "mean sector width" obtained separately from the daily HMF polarity observed when the Earth was located above (June 7 to December 6) or below (December 7 to June 6) the heliographic equator, it was found that statistically significant north-south differences of the HMF mean sector widths existed around the solar activity minimum, while no significant differences exist around the maximum or the solar polarity reversals. It was inferred, based on the sinusoidal HCS model, that the HCS would be displaced southward or northward from the heliographic equator during

the minimum phase, but it would be symmetric during the maximum phase [*Tritakis*, 1984], contrary to Rosenburg's inference.

The contrary inferences imply that the sinusoidal model cannot in general be used to adequately describe the warped HCS. It was confirmed by the middle of the 1980s that the warped HCS, at times symmetric and asymmetric relative to the heliographic equator, can be reliably modeled using the observed photospheric magnetic field and the potential field source surface (PFSS) model [*Hoeksema*, 1984 and references therein]. As shown by the modeled HCS for whole solar cycle [*Hoeksema*, 1984; 1992], the sinusoidal model may be valid only around solar activity minimum and during the declining phase of the cycle, and a sinusoidal model can be generized to fit either two or four sectors per rotation.

The definitive observational evidence of a southward HCS displacement of 10° from the heliographic equator was first obtained from Ulysses cosmic-ray observations in the rapid transit from the south to north solar poles between September 1994 and May 1995 [*Simpson et al.*, 1996]. The computed neutral line that agrees remarkably well with the set of HCS crossings observed by WIND and Ulysses during this interval is indeed displaced southward, with latitudinal excursions ranging from $-22°$ to $+17°$ [*Crooker et al.*, 1997]. An asymmetry of 10° in the HCS is expected to result in significantly different magnitudes of the radial field component in the positive and negative magnetic hemispheres. The HMF measured by Ulysses during the rapid transit did show a $\sim$ 10 % asymmetry, with the field strength in the south stronger than in the north. While suggestive, this asymmetry could be associated with temporal changes of the photospheric field because measurements made by Ulysses in the northern hemisphere were obtained near April 1995, several months later than measurements made in the southern hemisphere near December 1994 [*McComas et al.*, 2000]. To address this ambiguity, the magnetic field strength measured in positive and negative sectors by the WIND spacecraft in the ecliptic were compared. A large difference of 30% in the radial

component of the HMF was observed between December 1994 and April 1995, with a larger radial component in the south than in the north [*Smith et al.*, 2000]. This further confirms the southward displacement of the HCS during this interval.

By analyzing the occurrence fractions of the HMF at 1 AU directed toward and away from the Sun, Mursula and Hiltula (2003) found that during the last four solar minima between 1965 and 2001, the occurrence fractions for the HMF polarity prevalent in the northern heliographic hemisphere was found to be higher than the occurrence fractions in the southern hemisphere. They concluded that the average HCS was displaced southward during solar minimum times and that the temporary southward displacement of the HCS apparently observed during the Ulysses and WIND interval may be a persistent phenomenon. However, the large difference in radial HMF strength in positive and negative sectors observed by WIND tended to disappear after March 1995 (see Fig. 3 of *Smith et al.*, [2000]), implying that no significant southward displacement of the HCS existed between March and December, 1995.

A similar north-south asymmetry was also observed in the green line corona during a few solar minima, and the strong north-south asymmetry in the inner corona was found to be a persistent and repeated phenomenon [*Osherovich et al.*, 1999].

Does the noth-south displacement of the HCS occur in solar activity phases other than in minimum phase? How long do such north-south displacements last? What determines the north-south asymmetry in the global heliosphere?

To answer these questions and give a quantitative picture of the north-south displacement of the HCS we first develop, in the next section, an algorithm to quantitatively estimate the displacement of the source surface neutral line about the Sun's magnetic dipole equator and the heliographic equator. We analyze the factors that contribute to the north-south asymmetry on the basis of observations of the photospheric magnetic field and the PFSS model. In Section 3 we reproduce the 10° southward displacement of the HCS observed by ULYSSES and WIND, and compute

the positive-negative and north-south HCS displacement for the interval between 1976 and 2001. The causes of predicted positive-negative HCS displacement in various solar activity phases are discussed in section 4. Finally we summarize the results in Section 5.

2. Algorithm

It has been shown that the HCS location determined using the PFSS model agrees with in situ observations of sector boundaries as well as those computed using MHD models and better than those computed using the current sheet model [*Neugebauer et al.*, 1998]. The overall success rate of the HMF polarity predicted using the PFSS model and WSO data between June 1996 and June 2004 reaches as high as $84.5\% \pm 12.7\%$ [Zhao et al., 2005]. We develop the algorithm on the basis of the PFSS model.

In the PFSS model, the coronal field satisfies $\bigtriangledown \times B = 0$ out to a spherical "source surface" at $r = R_{ss} = 2.5R_{\odot}$ [*Hoeksema*, 1984], where the effect of the quasi-radial solar-wind outflow on the coronal magnetic field is simulated by assuming that the field is purely radial everywhere on the source surface. At the lower boundary, $r = R_{\odot}$, the radial field component is matched to the photospheric field, which is assumed to be radially oriented [*Wang and Sheeley*, 1992; *Zhao and Hoeksema*, 1993]. By definition, all field lines that extend from $r = R_{\odot}$ to the source surface at $r = R_{ss}$ are "open". The neutral line at the source surface and the open field regions at the coronal base derived using the PFSS model reproduce the global configuration of the HCS and coronal holes throughout the solar cycle fairly well [*Hoeksema*, 1984; *Wang et al*, 1996; *Zhao and Hoeksema*, 1999; *Zhao et al.* 2002]. Because of the various assumptions in the model it is not meaningful to assign a quantitative uncertainty to a particular location of the HCS. Confidence in the results is developed by validation of the results with observations.

2.1. Computation of the displacement of the HCS from the solar dipole equator and the heliographic equator

The observed displacement of the HCS southward from the heliographic equator during Carrington Rotation 1893 is shown in Figure 1. The negative source surface, most of which is located in the southern heliographic hemisphere in this rotation, is smaller than the positive source surface, most of which located in the northern heliographic hemisphere. To avoid any confusion with the northern (southern) heliographic hemisphere in the following discussion and to be valid in differnt solar cycles, we call the magnetic hemisphere with the same polarity as the dominant polarity in north (south) polar region the north (south) heliomagnetic hemisphere. This is always well defined and is quite obvious for all but one or two rotations around maximum when the HCS reaches the poles. The solid angles of south and north heliomagnetic hemispheres, Ω_{ss}^{S} and Ω_{ss}^{N}, can be expressed

$$\Omega_{ss}^{X} = \sum_{i=1}^{I^X} \delta\Omega_{ssi}, \tag{1}$$

where symbol X denotes N or S for north or south heliomagnetic hemisphere and I^X denotes I^N or I^S, the number of solid angle elements in the north or south heliomagnetic hemisphere. $\delta\Omega_{ssi}$ is the solid angle element. Using an equally spaced grid in ϕ and $cos\theta$ (ϕ and θ denote the Carrington longitude and colatitude, respectively, and $\Delta\phi = 2\pi/72$ and $\Delta(cos\theta) = 2/30$ for WSO data), each solid angle element has the same size, $\delta\Omega_{ssi} = \Delta(cos\theta) \cdot \Delta\phi = 4\pi/2160 = \delta\Omega_{ss}$. Equation (1) becomes

$$\Omega_{ss}^{X} = I^X \delta\Omega_{ss}. \tag{2}$$

The north and south solid angles for a warped HCS may be estimated using the idealized heliomagnetic equator (Zhao and Hundhausen, 1981), i.e., a flat HCS displaced by λ_m from the Sun's magnetic dipole equator (the antisymmetry plane of the Sun's

dipolar field),

$$\Omega_{ss}^{N} = 2\pi(1 - \sin\lambda_m), \tag{3}$$

and

$$\Omega_{ss}^{S} = 4\pi - \Omega_{ss}^{N}, \tag{4}$$

where $\lambda_m < 0$ if the HCS is displaced southward from the dipole equator.

Based on Equations (3) the effective displacement of the HCS from the Sun's magnetic dipole equator can be calculated,

$$\lambda_m = sin^{-1}(1 - \frac{\Omega_{ss}^{N}}{2\pi}) = sin^{-1}(1 - \frac{\delta\Omega_{ss}}{2\pi} I^{N}). \tag{5}$$

The HMF is largely determined by lower multipole magnetic moments of the photospheric magnetic field. The Sun's magnetic dipole defines a tilt angle, δ, relative to the Sun's rotation axis. The displacement of the HCS from the heliographic equator, λ, is thus

$$\lambda = \lambda_m |\cos\delta|. \tag{6}$$

Here the tilt angle of the Sun's magnetic dipole

$$\delta = \tan^{-1}\frac{\sqrt{g_{11}^2 + h_{11}^2}}{g_{10}}, \tag{7}$$

where g_{10}, g_{11} and h_{11} are the first degree spherical harmonic coefficients, and can be obtained using the global distribution of the radial photospheric magnetic field. The tilt angle increases from near 0° at sunspot minimum through 90° at maximum to 180° at the next minimum; it then returns to 0° in the next next minimum. The magnetic polarity in the south (north) heliomagnetic hemisphere also reverses around sunspot maximum from one solar cycle to the next, and is negative (positive) when $g_{10} > 0$ and positive (negative) when $g_{10} < 0$.

2.2. Estimate of the difference of the mean field between north and south heliomagnetic hemispheres

The radial HMF has been shown to be latitude independent, suggesting that the radial HMF is uniform in each heliomagnetic hemisphere [*Smith*, 1995]. The mean source surface field of each heliomagnetic hemisphere may be used to represent the relative uniform radial HMF in the corresponding heliomagnetic hemisphere, even though the source surface field predicted using the PFSS model is latitude and time dependent.

The total source surface area and the total source surface magnetic flux in the south and north heliomagnetic hemispheres are given by

$$A_{ss}^{X} = I^{X} R_{ss}^{2} \delta\Omega_{ss}, \tag{8}$$

$$\Phi_{ss}^{X} = R_{ss}^{2} \delta\Omega_{ss} \sum_{i=1}^{I^X} B_{ssi}^{X}, \tag{9}$$

where B_{ssi}^{X} denotes the source surface field strength in the solid angle element i. The mean source surface field strength over south and north heliomagnetic hemispheres is

$$\overline{B_{ss}^{X}} = \frac{\Phi_{ss}^{X}}{A_{ss}^{X}} = \frac{\sum_{i=1}^{I^X} B_{ssi}^{X}}{I^{X}}. \tag{10}$$

Since the total magnetic flux in the south heliomagnetic hemisphere must be equal to the total magnetic flux in the north heliomagnetic hemisphere, the ratio of the mean field over the south hemisphere to the mean field over the north hemisphere can be estimated by

$$\xi = \frac{\overline{B_{ss}^{S}}}{\overline{B_{ss}^{N}}} = \frac{I^{N}}{I^{S}}. \tag{11}$$

2.3. The causes of the north-south asymmetry of the HMF

As shown by Eq. (5), the north-south displacement of the HCS is determined by the total north and south source surface solid angles, Ω_{ss}^{N} and Ω_{ss}^{S}. Here Ω_{ss}^{X} depends on

the corresponding total solar surface solid angle Ω^X_{fp} and the mean expansion factor ϵ^X from $R_\odot$ to R_{ss}, i.e.,

$$\Omega^X_{ss} = \epsilon^X \Omega^X_{fp}. \tag{12}$$

Thus the north-south displacement of the HCS from the dipole equator depends on the mean expansion factor ϵ^N and the total solar surface solid angle Ω^N_{fp} of the heliomagnetic hemisphere with the polarity corresponding to that of the north polar field as follows

$$\lambda_m = sin^{-1}(1 - \frac{\epsilon^N \Omega^N_{fp}}{2\pi}). \tag{13}$$

Here ϵ^N and Ω^N_{fp} may be obtained by

$$\epsilon^N = \frac{\overline{B^N_{fp}}}{\overline{B^N_{ss}}} \left(\frac{R_\odot}{R_{ss}}\right)^2, \tag{14}$$

and

$$\Omega^N_{fp} = \frac{A^N_{fp}}{R^2_\odot} = \frac{\sum_i^{I^N} \delta A^N_{fpi}}{R^2_\odot} \tag{15}$$

The mean foot-point field B^N_{fp} in Equation (14) can be calculated by

$$\overline{B^N_{fp}} = \frac{\sum_i^{I^N} B^N_{fpi} \delta A^N_{fpi}}{A^N_{fp}} = \frac{\sum_i^{I^N} B^N_{fpi} \delta A^N_{fpi}}{\sum_i^{I^N} \delta A^N_{fpi}}, \tag{16}$$

where B^N_{fpi} is the field strength at the foot-point of a open field line that connects to the source surface field strength B^N_{ssi}. The elemental foot-point area in Equations (15) and (16) is

$$\delta A^N_{fpi} = \frac{B^N_{ssi}}{B^N_{fpi}} R^2_{ss} \delta\Omega_{ss} \tag{17}$$

3. The computation of the north-south asymmetry of the HMF

To estimate the north-south HCS displacement about the heliographic equator, λ, we need to estimate the north-south HCS displacement about the Sun's dipole equator, λ_m, and the tilt angle of the Sun's magnetic dipole, δ, as shown by Eqs. (5), (6) and (11). We extrapolate the observed photospheric field into the corona using the PFSS

model. For the photospheric field measurements, we employ Carrington synoptic charts from the Wilcox Solar Observatory (WSO) from May 1976 to Dec. 2001. We correct for the saturation of the Fe I 5250 Å line profile by multiplying the measured magnetic fluxes by the colatitude (θ) dependent factor $4.5 - 2.5\cos^2\theta$ [*Wang and Sheeley*, 1995].

3.1. Reproduction of the north-south HCS displacement between 23 Feb. and 23 March, 1995

Using the WSO synoptic chart for Carrington Rotation 1893 (23 Feb. – 23 March, 1995) and the PFSS model, the calculated source surface neutral line agrees remarkably well with the set of HCS crossings observed by WIND and Ulysses [Crooker et al., 1997]. This successful reproduction of the HMF sector structure validates this WSO synoptic chart and the PFSS model. We first obtain the spherical harmonic coefficients using this synoptic chart, and then calculate Sun's magnetic dipole tilt angle and the magnetic field at the source surface. The magnetic polarity in the southern (northern) heliomagnetic hemisphere is negative (positive) in 1995 (Figure 1). We have $I^N = 1275$, $I^S = 885$, $\delta = 8.38°$, and obtain $\lambda_m = -10.40$, $\lambda = -10.29$, and $\xi = 1.44$. The calculated displacement is the same as that inferred from Ulysses cosmic-ray observations in the first rapid transit [*Simpson*, 1996] and the calculated mean source surface field ratio of 1.44 is also nearly the same as that inferred from WIND observations of the HMF in the ecliptic, i.e., $3.5/2.5 = 1.40$ [*Smith et al.*, 2000].

All these successes in reproducing the HMF sector structure, the 10° of southward HCS displacement, and the 1.40 ratio of the mean radial HMF lead us to determine the north-south displacement of HCS for other Carrington Rotations with more confidence.

3.2. Prediction of north-south HCS displacement between 1976 and 2001

Figure 2 displays computations of Sun's magnetic dipole tilt angle (the top panel), the difference in the source surface solid angles between positive and negative

heliomagnetic hemispheres (the second panel), the north-south displacement of the HCS from Sun's dipolar equator and from the heliographic equator (the third panel), and the difference in the mean radial HMF amplitude between positive and negative heliomagnetic hemispheres (the bottom panel).

The top panel shows that at the solar minima around 1986 and 1996 the dipole tilt angle was $\sim 180^\circ$ and $\sim 0^\circ$, respectively, indicating that the magnetic polarity in southern polar cap was positive in 1986 and negative in 1996.

The second panel shows that the difference in the source surface solid angles between the positive and negative heliomagnetic hemispheres is almost always different from zero, i.e., the solid angles of the two hemispheres almost always differ from each other. This means that a north-south HCS displacement from the solar dipole equator is not an unusual phenomenon. A difference greater than 1.0 steradian in source surface solid angle between the two heliomagnetic hemispheres occurs in all phases of the solar activity cycle. As indicated by vertical dotted lines in Figure 2, there are two long intervals when most of the difference are greater than 1.0. Between March 1983 and July 1986 the solid angle of the negative (north) hemisphere is always greater than that of the positive (south) hemisphere, implying that the HCS is always displaced toward the positive (south) hemisphere from Sun's magnetic dipole equator. Between April 1992 and May 1995 the solid angle of the positive (north) hemisphere is always greater than that of the negative (south) hemisphere, implying that the HCS is always displaced toward negative (south) hemisphere. The HCSs for the two long intervals are both displaced southward, as shown in Panel 3 of Figure 2. The north-south HCS displacement about the heliographic equator is also shown in the panel. This prediction is consistent with the statistical result of Mursula and Hiltula [2003]. During other periods of time the difference in solid angle between the two heliomagnetic hemispheres and the HCS displacement from the magnetic dipole equator change frequently and the duration may be only a few or even a couple of solar rotations. Significant displacement

of the HCS about the magnetic dipole equator occurs also around solar activity maximum; However, there is no significant displacement about the heliographic equator because the dipole tilt angle approaches 90° around solar activity maximum.

The bottom panel of Figure 2 shows the difference in the predicted radial HMF field strength averaged over positive and negative heliomagnetic hemispheres. The prediction between April 1992 and May 1995 is consistent with the observation of WIND [*Smith*, 2000], showing that the southward HCS displacement does not continuously extend into sunspot minimum during this cycle.

4. Understanding the north-south HCS displacement

As mentioned in Section 1, the north-south HCS displacement has been invoked to understand the in-ecliptic detection of any heliographic latitude dependence in the dominant HMF polarity. Many hypotheses have been proposed to explain the formation of the HCS north-south displacement. For example, asymmetric activity between solar hemispheres, different solar wind plasma pressure resulting from asymmetric activity, unequal solar wind velocity in the two hemispheres, or the effect of interaction regions on the north-south displacement of the HCS [*Tritakis*, 1984 and the references therein]. The role of coronal holes in the formation of the HCS displacement was recognized on the basis of the observation of coronal holes, i.e., the inclination and shape of the sector boundaries depend very much on the number, polarities, and relative positions of coronal holes and open field regions [*Burlaga et al.*, 1978]. *Osherovich et al* [1984] related the north-south inner coronal asymmetry to the existence of a significant quadrupole term in the global photospheric magnetic field. The role of the strong quadrupole component in producing the north-south asymmetry was also suggested in study of nonradial coronal streamers [*Wang*, 1996].

The southward displacement of the HCS observed by the Ulysses and WIND spacecraft in the descending phase has been attributed to the north-south asymmetry

in the Sun's polar magnetic field [Jokipii and Smith, 1998]. The photospheric magnetic field can be expanded as multipoles and the HMF is composed mainly of the lower multipole components: the dipole, the quadrupole, the hexapole and the octupole. Around sunspot minimum these low order multipoles are oriented basically parallel to the Sun's rotation axis, and can be approximately represented by the zonal harmonic coefficients g_{10}, g_{20}, g_{30}, and g_{40}. The polar field represented by g_{10} and g_{30} has opposite polarity in north and south polar regions, but the field described by g_{20} and g_{40} has the same polarity in both polar regions, giving rise to an asymmetry in the field strength. The north-south asymmetry in the heliosphere around sunspot minimum is thus also attributed to the existence of a significant quadrupole term, g_{20}, in the global magnetic field of the Sun [*Bravo and Gonzalez-Esparza*, 2000]. The polar magnetic field is greater (less) in the south polar region than in the north if g_{10} and g_{20} have opposite (identical) sign. Thus by comparing g_{10} and g_{20} we might easily figure out which polar cap has stronger mean field strength if the contribution of the octupole, g_{40}, and other higher order terms may be neglected.

The top panel of Figure 3 (see also http://sun.stanford.edu/wso/gifs/polar.gif) shows the time (Carrington Rotation) variation of the difference in the observed WSO field between north and south polar caps above 55° of north and south heliographic latitude. Each point in the panel denotes the rotation-averaged value of the north polar field subtracted by the rotation-averaged value of the south polar field. The polar cap imbalance in the field strength, i.e., the north-south asymmetry in the Sun's polar magnetic field, occurs in all solar activity phases. Each specific north-south asymmetry usually lasts more than 10 solar rotations. The annual variation of the north-south asymmetry in the Sun's polar magnetic field is associated with the contamination from the polar field visibility imbalance.

The second panel of Figure 3 displays the time variation of the amplitude and sign of the zonal low-order multipole components, g_{10}, g_{20} and g_{40} between May 1976 and

December 2001. The opposite sign between g_{10} and g_{20} from April 1992 to May 1995 may be used to explain the greater field strength in southern polar cap. However, this does not explain the interval from March 1983 to July 1986 and others. For example, in the periods between CR1705 and CR1720, between CR1732 and CR1755, and between CR1850 and CR1862, the contribution of the octupole g_{40} actually dominates over the quadrupole g_{20}. This indicates that the contribution of the octupole as well as the quadrupole to the polar field should be taken into consideration to understand the north-south asymmetry in the Sun's polar magnetic field.

Is the north-south asymmetry in the Sun's polar magnetic field the necessary and sufficient condition for the occurrence of the HCS displacement? If this were the case, HCS displacements with duration greater than 10 solar rotations would be expected to occur in all solar activity phases, corresponding to the polar magnetic field asymmetry shown in the top panel. The bottom panel of Figure 3 shows the computed HCS displacement relative to the Sun's magnetic dipole equator. There are only two long intervals in the late declinning and minimum phases when the HCS displacement corresponds to the polar magnetic field asymmetry. There is no HCS displacement that lasts more than 10 solar rotations in the other solar activity phases. This implies that the north-south asymmetry in the Sun's polar magnetic field is not the sufficient condition for the occurrence of a HCS displacement.

As shown in Equation (13), in addition to the total solar surface solid angle that is associated with the mean field in open field regions such as polar coronal holes, the mean expansion factor of open field regions in the northern or southern hemisphere from the solar surface to the source surface must be taken into consideration to explain the quantitative picture of the north-south displacement of the HCS from Sun's magnetic dipole equator. Panel 3 of Figure 3 displays the difference between the mean expansion factors of open field regions in the positive and negative heliomagnetic hemispheres. Around solar activity minimum the mean expansion factors are basically identical

between the two hemispheres, but significant difference occurs around the maxima in 1980, 1990 and 2000. Thus around solar activity minimum the HCS displacement is determined basically by the area asymmetry between north and south polar open field regions or by the polar field strength asymmetry, because around solar activity minimum there are no low latitude coronal holes and the expansion factor for the two polar open field regions are basically the same. However, in other solar activity phases the expansion factor should be taken into consideration. One example is CR1740 when both g_{20} and g_{40} are parallel with g_{10} (the second panel). The mean northern polar field is greater than the southern polar field, but the HCS is still displaced southward. In this case the asymmetry in expansion factors of the open field regions is the major factor in determining the north-south HCS displacement.

Figure 4 shows another example that illustrates the importance of the north-south asymmetry in the expansion factors between positive and negative open field regions. The example shows no displacement of the HCS for CR1733, even though there is asymmetry in the area and field strength between the north and south open field regions. The example illustrates that during this period of time, low-latitude open field regions occur frequently, and the number of low-latitude open field regions in the two hemispheres are usually not the same; their expansion factors differ significantly, and this becomes one of the major factors in determining the north-south HCS displacement in the period of time.

5. Summary and discussion

By comparing the solid angles occupied by positive polarity and negative polarity on the source surface we develop an algorithm to quantitatively estimate the north-south HCS displacement about the Sun's magnetic dipole equator and the heliographic equator. The southward HCS displacement from the heliographic equator and the ratio of the mean source surface field strength between the two hemispheres computed for

Carrington Rotation 1893 quantitatively agree with the observations of Ulysses and WIND. This good reproduction of the north-south HCS displacement strengthens our confidence in the prediction of the north-south HCS displacement for the 362 Carrington rotations between 1976 and 2001.

The HCS displacements determined over the 25 years considered here show that a north-south HCS displacement is a normal phenomenon. North-south HCS displacements of a few degrees from the Sun's magnetic dipole equator occur during almost the entire solar activity cycle. Most of the HCS displacements last only a few solar rotations. Around solar activity maximum the north-south HCS displacement from the heliographic equator is quite insignificant, and significantly different from the HCS displacement relative to the Sun's magnetic dipole equator because the Sun's magnetic dipole is nearly perpendicular to the Sun's rotation axis and the magnetic configuration is less dipole like.

There are two long southward HCS displacement intervals lasting more than three years. These occur between March 1983 and July 1986 and between April 1992 and May 1995, in the declining phase of the solar activity cycle, close to the minimum. During these intervals the HCS displacement from the heliographic equator is virtually the same as the HCS displacement from the Sun's magnetic dipole equator because the Sun's magnetic dipole axis is aligned parallel or anti-parallel to the Sun's rotation axis. Such displacements of several to more than ten degrees may lead to the total disappearance of the HMF sector structure in the ecliptic near sunspot minimum, as reported many years ago [*Wilcox*, 1972]. This is not due to a solar monopole but to the factors we have described in this paper. In the four solar minima covered by near-ecliptic in situ observations of the HMF, the heliographic latitude dependence of the dominant HMF sector observed near the highest heliographic latitude shows a systematically stronger development in the northern heliographic hemisphere than in the south [*Mursula and Hiltula*, 2003]. The asymmetric green-line corona was also observed around solar activity

minimum in a few solar cycles[*Osherovich, et al.*, 1999]. All of these investigations unambiguously support *Mursula and Hiltula* [2003] conclusion that the southward HCS displacement around solar activity minimum is a persistent pattern.

Because of the long duration of the southward displacement of the HCS around solar activity minimum, it is possible to detect its existence from the study of sectors observed near the Earth's highest heliographic latitudes. The same technique is expected to be far less sensitive to the predicted existence of the short lived north-south HCS displacements in the solar activity phases other than around the solar activity minimum. Thus such results may not be used to deny the existence of short lived north-south HCS displacements. To determine whether or not the prediction of the HCS displacements is valid, it is necessary to search elsewhere for the observational evidence of the predicted HCS displacements. This is especially true for the short lived HCS displacements because it may not be ruled out that the short lived HCS displacements might be associated with the polar field visibility imbalance.

The HMF comes from open field regions in the solar corona. Thus any asymmetry of the heliosphere about the Sun's magnetic dipole equator must be, in general, associated with the characteristics of open field regions, such as the areas (or field strengths) and the outward expansion factor of open field regions. Around solar activity minimum the computed mean expansion factors of open field regions in the north and south heliomagnetic hemispheres are basically the same, so the asymmetry in area or field strength of open field regions is the major factor that determines the north-south HCS displacement. This is consistent with what has been suggested by *Jokipii and Smith*, [1998]. It should be noted that both the octupole g_{40} and the quadrupole g_{20} must be taken into consideration in examining the north-south asymmetry of the polar field, even around solar activity minimum.

For the HCS displacements that occurred in solar activity phases other than the declining and minimum phases, the role of the expansion factor becomes more

important, sometimes dominating over the influence of the area or field strength of open field regions. The reason is that during the other activity phases the geometry of the open field regions is more variable. The observed low-latitude coronal holes sometimes dominate over polar coronal holes and the number and size of low-latitude coronal holes are often asymmetric about the heliographic equator; this implies the existence of asymmetry in the characteristics of coronal holes in these activity phases.

6. Acknowledgements

This work was supported by NASA grants NNG04GB87, NAG5-13261, and NNG05GH14G

References

Bravo S. and J. A. Gonzalez-Esparza, The north-south asymmetry of the solar and heliospheric magnetic field during activity minima, *Geophys. Res. Lett., 27*, 847, 2000.

Burlaga, L. F., K. W. Behannon, S. F. Hansen, G. W. Pneuman, and W. C. Feldman, Sources of magnetic fields in recurrent interplanetary streams, *J. Geophys. res., 83*, 4177, 1978.

Crooker, N. U., A. J. Lazarus, J. L. Phillips, J. T. Steinberg, A. Szabo, R. P. Lepping, and E. J. Smith, Coronal streamer belt asymmetries and seasonal solar wind variations deduced from Wind and Ulysses data, *J. Geophys. Res., 102*, 4673-4679, 1997.

Hoeksema, J. T., Structure and evolution of the large scale solar and heliospheric magnetic fields, Ph.D. thesis, Stanford Univ., 1984.

Hoeksema, J. T., Evaluation of the solar and coronal field structure: 1976-1991, in *Solar Wind Seven*, ed. E. Marsh and R. Schwenn (Oxford: Pergamon), pp. 191-196, 1992.

Hundhausen, A. J., An interplanetary view of coronal holes, in *Coronal Holes and High Speed Solar Wind Streams*, edited by J. B. Zirker, P. 298, Colorado University Press, Boulder, Colo., 1977.

Jokipii, J. R. and E. J. Smith, Global north-south asymmetry of the heliospheric magnetic field and cosmic ray, in *EOS Transaction, 79*, No. 17, pp.S276, 1998.

McComas, D. J., B. L. Barraclough, H. O. Funsten, J. T. Gosling, E. Santiago-Munoz, R. M. Skoug, B. E. Goldstein, M. Neugebauer, P. Riley, and A. Balogh, Solar wind observations over Ulysses' first full polar orbit, *J. Geophys. Res., 105*, 10419-10433, 2000.

Mursula, K. and T. Hiltula, Bashful ballerina: Southward shifted heliospheric current sheet, Geophys. Res. Lett., 30 (22), p. SSC 2–1-4, doi: 10.1029/2003GL018201,

2003.

Neugebauer, M., et al., Spatial structure of the solar wind and comparisons with solar data and models,*J. Geophys. Res., 103*, 14587, 1998.

Rosenberg, R. L., Unified theory of the interplanetary magnetic field, *Solar Phys., 15*, 72, 1970.

Rosenberg, R. L., Heliographic latitude dependence of the IMF dominant polarity in 1972-1973 using Pioneer 10 data, *J. Geophys. Res., 80*, 1339, 1975.

Rosenberg, R. L. and J. Coleman, Jr., Heliographic latitude dependence of the IMF dominant polarity of the interplanetary magnetic field, *J. Geophys. Res., 74*, 5611, 1969.

Schulz, M., Interplanetary sector structure and the heliomagnetic equator, *Astrophys. Space Sci., 24*, 371, 1973.

Simpson, J. A., M. Zhang and S. Bame, A solar polar north-south asymmetry for cosmic-ray propagation in the heliosphere: The Ulysses pole-to-pole rapid transit, *Astrophys. J., 465*, L69-L72, 1996.

Smith, E. J., B. T. Tsurutani, and R. L. Rosenberg, Observations of the interplanetary sector structure up to heliographic latitudes of 16°: Pioneer 11, *J. Geophys. Res., 83*, 717, 1978.

Smith, E. J., J. R. Jokipii, J. Kota, R. P. Lepping, and A. Szabo, Evidence of a north-south asymmetry in the heliosphere associated with a southward displacement of the heliospheric current sheet, *Astrophys. J., 533*, 1084-1089, 2000.

Osherovich, V. A., I. Tzur, and E. B. Gliner, Theoretical model of the solar corona during sunspot minimum: 1. Quasi-static approximation, *Astrophys. J., 284*, 412-421, 1984.

Osherovich, V. A., J. Fainberg, R. R. Fisher, S. E. Gibson, M. L. Goldstein, M. Guhathakurta and E. Siregar, The north-south asymmetry with inferred magnetic quadrupole, in *Solar Wind Nine* edited by S. R. Habbal, R. Esser, J.

V. Hollweg, and P. A. Isenberg, The American Institute of Physics, p. 721, 1999.

Tritakis, V. P., Heliospheric current sheet displacements during the solar cycle evolution, *J. Geophys. Res., 89*, A8, 6588, 1984.

Wang, Y.-M., Nonradial coronal streamers, *Astrophys. J., 456*, L119-L121, 1996.

Wang, Y.-M. and N. R. Sheeley, Jr., On potential field models of the solar corona, *Astrophys. J., 392*, 310-319, 1992.

Wang, Y.-M. and N. R. Sheeley, Jr., Solar implications of Ulysses interplanetary field measurements, *Astrophys. J., 447*, L143-L146, 1995.

Wang, Y.-M., S. H. Hawley, and N. R. Sheeley, Jr., The magnetic nature of coronal holes, *Science, 271*, 464-469, 1996.

Wilcox, J. M., Why does the Sun sometimes look like a magnetic monopole, Comments on Astrophys. and Space Phys., 4, 141, 1972.

Wilcox, J. M. and N. F. Ness, Quasi-stationary corotating structure in the interplanetary medium, *J Geophys. Res., 70*, 5793, 1965.

Zhao, X. P. and A. J. Hundhausen, Organization of solar wind plasma properties in a tilted,heliomagnetic coordinate system, *J Geophys. Res., 86*, 5423, 1981.

Zhao, X. P. and J. T. Hoeksema, Unique determination of model coronal magnetic fields using photospheric observations, *Solar Phys. 143*, 41, 1993.

Zhao, X. P., J. T. Hoeksema, and P. H. Scherrer, Changes of the boot-shaped coronal hole boundary during Whole Sun Month near sunspot minimum, *J. Geophys. Res., 104*, 9735-9751, 1999.

Zhao, X. P., J. T. Hoeksema, and N. B. Rich, Modeling the radial variation of coronal streamer belts during ascending activity phase, *Advances in Space Research, 29*, No. 3, p.411, 2002.

Zhao, X. P., J. T. Hoeksema, Y. Liu, and P. H. Scherrer, The success rate of predicting the heliospheric field polarity with MDI synoptic charts, *J. Geophys. Res.,*, submitted, 2005

X. P. Zhao, W. W. Hansen Experimental Physics Laboratory, Stanford University, Stanford, CA 94305-4085. (e-mail: xpzhao@solar.stanford.edu)

J. T. Hoeksema, W. W. Hansen Experimental Physics Laboratory, Stanford University, Stanford, CA 94305-4085. (e-mail: hthoeksema@solar.stanford.edu)

P. H. Scherrer, W. W. Hansen Experimental Physics Laboratory, Stanford University, Stanford, CA 94305-4085. (e-mail: phscherrer@solar.stanford.edu)

Received _____

Third Version: 1 march 2005

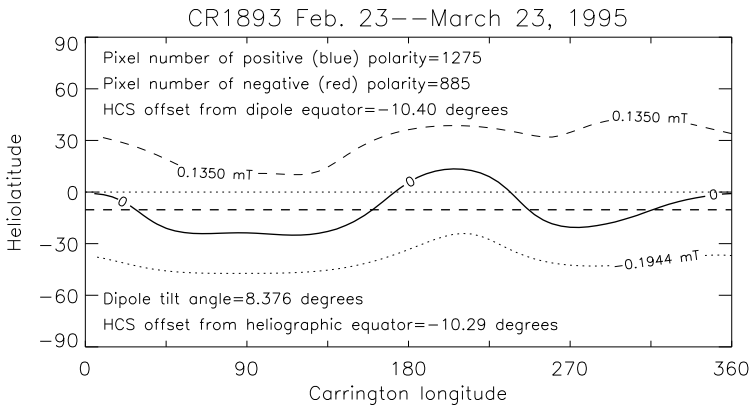

Figure 1. The computed neutral line (the thick solid curve) and its southward displacement (the thick dashed line) from the heliographic equator (the dotted line) for Carrington Rotation 1893.

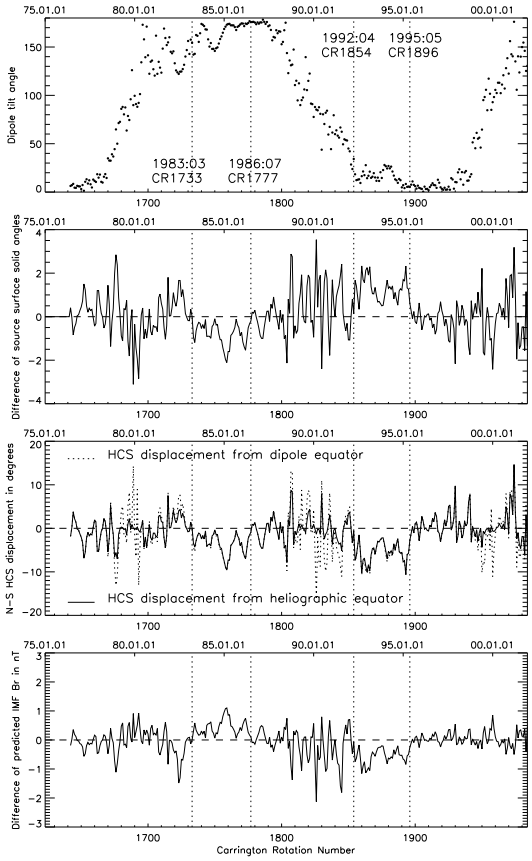

Figure 2. The Sun's magnetic dipole tilt angle (the top panel), the difference in the source surface solid angle between positive and negative hemispheres (the second panel), the displacement of the HCS from dipole and heliographic equators (the third panel), and the difference in field amplitude between positive and negative heliomagnetic hemispheres from 1976 to 2001.

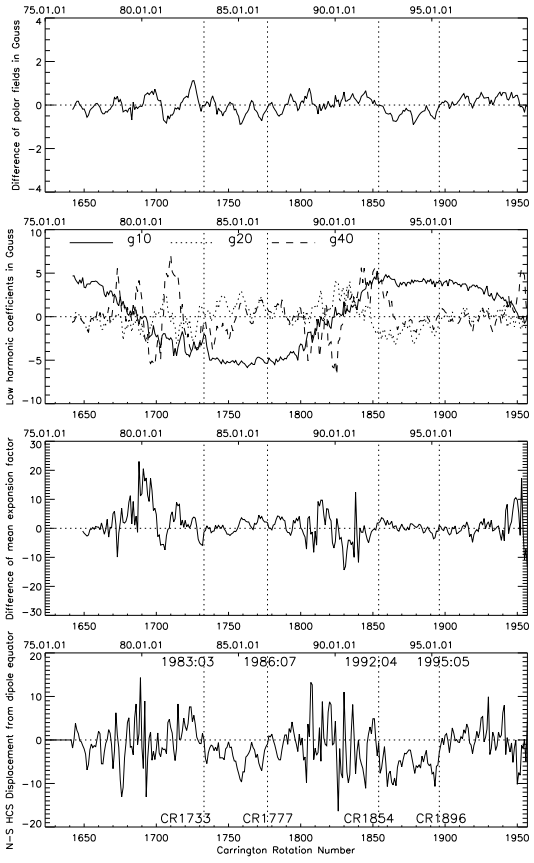

Figure 3. The association of north-south displacement of the HCS from the Sun's magnetic dipole equator (the bottom panel) with the difference in WSO mean field amplitude between north and south polar caps (the top panel), the rotation-axis-aligned dipole, quadrupole and octupole, g10, g20 and g40 (the second panel), and the difference in mean expansion of open field regions between positive and negative hemispheres.

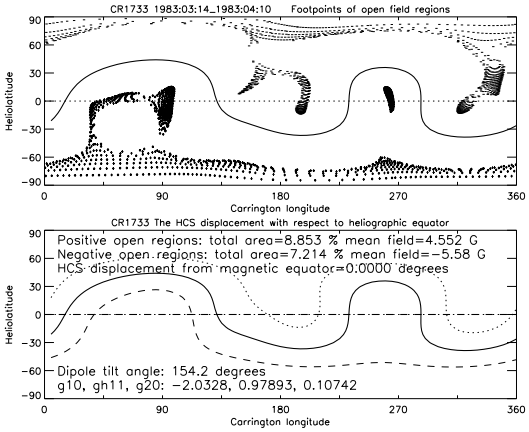

Figure 4. The positive (+) and negative (−) open field regions (the first panel) and the neutral line (the thick solid line) and its displacement (the dashed line) from the heliographic equator (the dotted line in the second panel) for Carrington rotations 1733.